

# Meson Assisted Strange Dibaryons

A. Gal

*Racah Institute of Physics, The Hebrew University, 91904 Jerusalem, Israel*

---

## Abstract

The state of the art in dibaryons with strangeness is reviewed, including the  $K^-pp$  dibaryon which signals the onset of  $\bar{K}$ -nuclear binding. A new type of strange dibaryons is highlighted, where the primary binding mechanism is provided by strong  $p$ -wave pion interactions, as demonstrated by a quasibound ( $I = \frac{3}{2}$ ,  $J^P = 2^+$ )  $\pi YN$  dibaryon calculation.

---

## 1. Introduction

The quark model (QM) has been very successful in reproducing SU(3) flavor octet (**8**) and decuplet (**10**) baryon masses, and to a somewhat lesser extent also higher mass baryon resonances, in terms of three-quark ( $3q$ ) configurations. It is remarkable then that subsequent predictions of  $6q$  configurations of bound or quasibound dibaryons have not been found to be realized in Nature, and that todate there is not even one single unambiguously established dibaryon. This statement is challenged by recent indications from  $np \rightarrow d\pi\pi$  reactions at CELSIUS-WASA of a resonance structure at  $M_R \approx 2.37$  GeV and  $\Gamma_R \approx 70$  MeV that could be interpreted as a  $\Delta\Delta$  dibaryon bound by about 100 MeV, but still about 200 MeV above the  $d\pi\pi$  threshold [1]. We note that quark cluster calculations for  $L = 0$   $6q$  configurations [2] come up with only a weakly bound  $(I, J^P) = (0, 3^+)$   $\Delta\Delta$  dibaryon which in terms of a  $NN$  configuration corresponds to a high-lying  ${}^3D_3$   $pn$  resonance.

In the strange sector, Jaffe's dibaryon  $H$  with strangeness  $\mathcal{S} = -2$  and quantum numbers  $(I, J^P) = (0, 0^+)$  which was predicted as a genuinely bound state well below the  $\Lambda\Lambda$  threshold, perhaps the most cited ever prediction made for any dibaryon [3], has not been confirmed experimentally in spite of several comprehensive searches [4]. Another equally ambitious early prediction was made by Goldman *et al.* [5], also using a variant of the MIT bag

model, for  $\mathcal{S} = -3$  dibaryons with  $(I, J^P)$  values  $(\frac{1}{2}, 1^+)$  and  $(\frac{1}{2}, 2^+)$ , dominated by  $\Omega N$  structure and lying below the  $\Xi\Lambda$  threshold. More realistic quark cluster calculations by Oka *et al.* [6], applying resonating group methods, did not confirm Jaffe's deeply bound  $H$ , placing it just below the  $\Xi N$  threshold as a resonance about 26 MeV above the  $\Lambda\Lambda$  threshold. The underlying binding mechanism common to all of these orbital angular momentum  $L = 0$  configurations is the color-magnetic gluon exchange interaction between quarks, a feature emphasized by Oka [7] who systematically studied  $L = 0$  dibaryon configurations that could benefit from short-range attraction. Following earlier quark cluster calculations [2, 6], these calculations resulted in no strange dibaryon bound states, and for the  $\Omega N$ -dominated  $\mathcal{S} = -3$  bound-state configurations predicted in Ref. [5], in particular, only a  $(I, J^P) = (\frac{1}{2}, 2^+)$  quasibound state resulted.

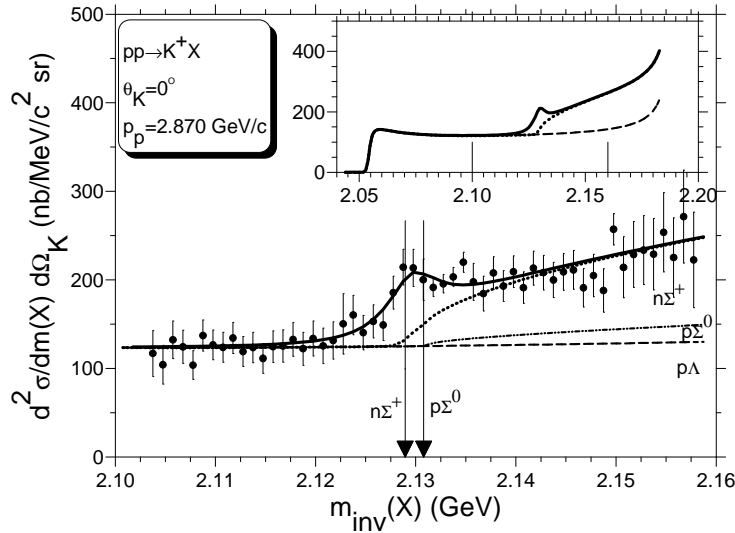


Figure 1:  $YN$  invariant mass spectrum taken by the HIRES Collaboration at COSY [14] around the  $\Sigma N$  threshold. The solid curve is a combined fit to  $pp \rightarrow K^+(\Lambda p, \Sigma^0 p, \Sigma^+ n)$ , including a BW fit to the threshold cusp.

For strangeness  $\mathcal{S} = -1$ , the focus of this review, old  $K^- d \rightarrow \pi^- \Lambda p$  data [8] suggested resonant  $\Lambda p$  structures at the  $\Sigma N$  threshold and 10 MeV above it. However, a  $(I, J^P) = (\frac{1}{2}, 1^+)$   $\Sigma N$  quasibound state is not necessarily required in order to reproduce the general shape of the  $\Lambda p$  spectrum, as shown by multichannel Faddeev calculations [9, 10]. A cusp-like structure at

the  $\Sigma N$  threshold region could arise from the particularly strong one pion exchange tensor interaction in the  $\Lambda N - \Sigma N$  coupled-channel  ${}^3S_1 - {}^3D_1$  partial waves. Several low-lying  $L = 1$   $\Lambda N$  resonances were predicted in singlet and triplet configurations in a QM study by Mulders *et al.* [11], but negative results, particularly for the singlet resonance, were reported in dedicated  $K^-$  initiated experiments [12, 13] near the  $\Sigma N$  threshold.  $YN$  invariant mass spectra taken in recent  $pp \rightarrow K^+ X$  experiments at COSY [14], shown in Fig. 1, give evidence for a cusp behavior at the  $\Sigma N$  threshold, but no further imminent structure below or above. The portion of the spectrum below the kinematical range spanned in Fig. 1 is shown in detail in Fig. 2, countering earlier evidence from Saturne [16] for a dibaryon signal at  $M_X = 2097$  MeV.

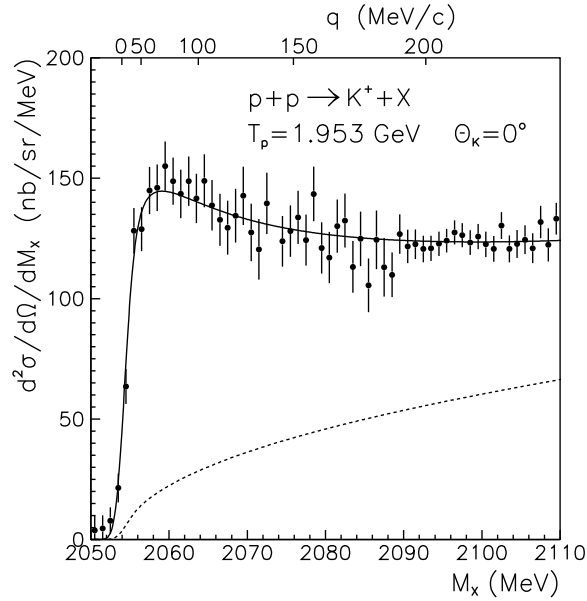


Figure 2:  $\Lambda N$  invariant mass spectrum below the  $\Sigma N$  threshold taken by the HIRES Collaboration at COSY [15].

In the present paper, following a brief summary of dibaryon theoretical expectations, I introduce the notion of pion assisted dibaryons,  $\pi BB'$ . The idea is to enhance the binding of a  $L = 0$   $BB'$  configuration through the strong attraction provided by  $p$ -wave  $\pi B$  resonances. For the  $\pi NN$  system this scenario requires quantum numbers ( $I = 2, J^P = 2^+$ ) to maximize the attraction from each one of the  $(3, 3)$  resonating  $\pi N$  subsystems, but then

the  $NN$  subsystem must have  $(I_{NN} = 1, J^P = 1^+)$  which is Pauli forbidden. Hence this mechanism fails for  $\mathcal{S} = 0$ , although  $(I = 2, J^P = 2^+)$  is allowed for a  $\pi NN$  configuration with  $(I_{NN} = 1, {}^{2s+1}L = {}^3P)$  and  $\ell_\pi = 0, 2, 4$ , and also for a  $\Delta N$  configuration, particularly in  $L = 0$ . Dibaryons of this sort that cannot be composed of two nucleons were discussed long ago in the QM and termed ‘extraneous dibaryons’ [17]. The lowest ones predicted are  $(I = 0, J^P = 0^-, 2^-)$  at  $M \approx 2120$  MeV, with the  $0^-$  subsequently assigned to a  $\pi NN$  resonance suggested by observed anomalies in  $(\pi^+, \pi^-)$  reactions on nuclei at  $T_\pi = 50$  MeV ( $M_{\pi NN} \sim 2065$  MeV) [18]. Such a state can be realized for two nucleons in  $(I_{NN} = 1, {}^{2s+1}L_J = {}^1S_0)$  plus an  $s$ -wave pion. There has been no solid experimental support for this dibaryon candidate ever since.

The limitations imposed by the Pauli principle in the  $\mathcal{S} = 0$  sector have no counterpart in the  $\mathcal{S} = -1$  sector, where a  $\pi\Lambda N$  stretched configuration  $(I = \frac{3}{2}, J^P = 2^+)$  is allowed. A possible quasibound state in this configuration has been recently studied [19, 20] by solving three-body Faddeev equations with  ${}^3S_1 - {}^3D_1$ ,  $\Lambda N - \Sigma N$  coupled channels chiral QM local interactions, and coupled  $\pi Y$  ( $Y \equiv \Lambda, \Sigma$ ) and  $\pi N$  separable  $p$ -wave interactions fitted to the position and decay parameters of the  $\Sigma(1385)$  and  $\Delta(1232)$  resonances, respectively. The results exhibit strong sensitivity to the  $p$ -wave  $\pi Y$  interaction, the least phenomenologically constrained interaction in this calculation, with a  $\pi\Lambda N$  quasibound state persisting over a wide range of acceptable parametrizations.

Finally, we briefly review the ongoing study, both theoretically and experimentally, of a more familiar example of meson assisted dibaryons: a  $K^-pp$  quasibound state in the  $\mathcal{S} = -1$  sector, driven by the  $\Lambda(1405)$  which within  $\bar{K}N - \pi\Sigma$  coupled channels appears as a  $s$ -wave  $K^-p$  quasibound state (QBS). For a recent overview of  $K^-pp$  and its implications to  $\bar{K}$ -nuclear QBS phenomenology, see Ref. [21],

## 2. Deuteron-like dibaryon candidates

Here we review  $BB'$  deuteron-like dibaryon candidate configurations made out of  $\mathbf{8}_f$  baryons in which no explicit quark degrees of freedom are considered. A well known example is the  $\mathcal{S} = 0$  ( $I = 0, J^P = 1^+$ )  $NN$  weakly bound deuteron. It is established experimentally that for  $\mathcal{S} = -1$ , the  $\Lambda N$  and  $\Sigma N$  interactions are too weak to provide binding. The associated scattering data have been used in several  $YN$  potential fits, respecting  $SU(3)_f$  within well de-

Table 1:  $\mathcal{S} = -2, -3, -4$  deuteron-like  $L = 0$  dibaryon candidates from the Nijmegen meson exchange model NSC97 [22] and from EFT predictions [23]. Plus means yes, minus means no.

Strangeness	$\mathcal{S} = -2$		$\mathcal{S} = -3$		$\mathcal{S} = -4$
$BB'$	$\Sigma\Sigma$	$\Lambda\Xi$	$\Sigma\Xi$	$\Xi\Xi$	
$(I, {}^{2s+1}[L = 0]_j)$	$(2, {}^1S_0)$	$(\frac{1}{2}, {}^1S_0)$	$(\frac{3}{2}, {}^1S_0)$	$(\frac{3}{2}, {}^3S_1)$	$(1, {}^1S_0)$
NSC97	+	−	+	+	+
EFT	−	+	+	−	+

finer symmetry breaking schemes, to make predictions for stranger  $BB'$  systems. There is almost general consensus, supported also by scarce  $\Lambda\Lambda$  data, that there are no bound states for  $\mathcal{S} = -2$ , except for a  $\Sigma\Sigma$  ( $I = 2, J^P = 0^+$ ) quasibound state. However, for  $\mathcal{S} = -3, -4$  there are several bound-state candidates, as listed in Table 1. The bound states listed in the table are due to two methodologies:

- The latest Nijmegen extended-soft-core (ESC) meson-exchange model, with broken  $SU(3)_f$  for  $\mathcal{S} = 0, -1, -2$ , claims no quasibound states (QBS) [24] while providing no predictions yet for stranger systems. Earlier soft-core versions, e.g. NSC97 [22], found QBS for  $\mathcal{S} = -3, -4$  as listed in Table 1. The three  ${}^1S_0$  bound states in this model are in one-to-one correspondence with  $BB'$  states assigned in  $SU(3)_f$  to the  $\mathbf{27}_f$  representation which includes the  $NN$   ${}^1S_0$  virtual state. Similarly, the  ${}^3S_1$  bound state in this model, as listed in the table, is also the only  $BB'$  state which together with the deuteron is assigned in  $SU(3)_f$  to the  $\overline{\mathbf{10}}_f$  representation.
- The Bonn-Jülich chiral effective field theory (EFT) model, applied in lowest order to  $\mathcal{S} = -1, -2, -3, -4$  with low energy constants (LEC) constrained by  $SU(3)_f$  and fitted to low-energy  $YN$  data [25] finds no

QBS for  $\mathcal{S} = -1$  and also for  $\mathcal{S} = -2$  [26]. The  $\mathcal{S} = -3, -4$  sectors require only the five LECs determined in the  $YN$  sector fit, independently of the sixth LEC required in the  $\mathcal{S} = -2$  sector (this LEC is consistent with zero). This is how one gets predictions [23] for the  $\mathcal{S} = -3, -4$  dibaryon candidates listed in Table 1. The predicted binding energies are all in the several MeV range, in agreement with what one expects for deuteron-like dibaryons where pion dynamics is dominant. The model dependence of these predictions is assessed within the model by varying a cutoff momentum in the range  $550 - 700$  MeV/c. Additional model dependence is likely to arise in next-to-leading-order evaluations. While the predictions of the EFT model differ for some states and agree for other ones with those of the NSC97 model, both these models predict strong attraction for all the configurations listed in the table.

### 3. Six-quark dibaryon configurations

Early discussions of  $6q$  dibaryons were based on symmetry considerations related to the assumed dominance of a color-magnetic (CM) gluon exchange interaction

$$V_{CM} = \sum_{i < j} -(\lambda_i \cdot \lambda_j)(s_i \cdot s_j)v(r_{ij}), \quad (1)$$

where  $\lambda_i$  and  $s_i$  are the color and spin operators of the  $i$ -th quark and  $v(r_{ij})$  is a flavor-conserving short-ranged spatial interaction between quarks  $i, j$ . For  $L = 0$  orbitally symmetric color-singlet  $n$ -quark cluster, the matrix element of  $v(r_{ij})$  is independent of the particular  $i, j$  pair and is denoted  $\mathcal{M}_0$ , allowing for a closed form summation over  $i$  and  $j$  in Eq. (1) with the result:

$$\langle V_{CM} \rangle = \left[ -\frac{n(10-n)}{4} + \Delta\mathcal{P}_f + \frac{s(s+1)}{3} \right] \mathcal{M}_0, \quad (2)$$

where  $\mathcal{P}_f$  sums over  $\pm 1$  for any symmetric/antisymmetric flavor pair,  $\Delta\mathcal{P}_f$  means with respect to the  $SU(3)_f$   $\mathbf{1}$  antisymmetric representation of  $n$  quarks,  $n = 3$  for baryons and  $n = 6$  for dibaryons,  $s$  is the total Pauli spin, and where  $\mathcal{M}_0 \sim 75$  MeV from the  $\Delta - N$  mass difference. The leading  $\mathcal{S} = 0, -1, -2, -3$  dibaryon candidates are listed in Table 2 following Ref. [7], where  $\Delta\langle V_{CM} \rangle$  stands for the CM interaction gain  $\langle V_{CM} \rangle_{6q} - \langle V_{CM} \rangle_B - \langle V_{CM} \rangle_{B'}$  in the  $6q$  dibaryon configuration with respect to the sum of CM contributions

Table 2: Leading  $6q$   $L = 0$  dibaryon candidates [7], their  $BB'$  structure and the CM interaction gain with respect of the lowest  $BB'$  threshold calculated by means of Eq. (2). Asterisks are used for the  $\mathbf{10}_f$  baryons  $\Sigma^* \equiv \Sigma(1385)$  and  $\Xi^* \equiv \Xi(1530)$ . The symbol  $[i,j,k]$  stands for the Young tableaux of the  $SU(3)_f$  representation, with  $i$  arrays in the first row,  $j$  arrays in the second row and  $k$  arrays in the third row, from which  $\mathcal{P}_f$  is evaluated.

$-\mathcal{S}$	$SU(3)_f$	$I$	$J^\pi$	$BB'$ structure	$\frac{\Delta\langle V_{CM} \rangle}{M_0}$
0	$[3,3,0] \overline{\mathbf{10}}$	0	$3^+$	$\Delta\Delta$	0
1	$[3,2,1] \mathbf{8}$	$1/2$	$2^+$	$\frac{1}{\sqrt{5}}(N\Xi^* + 2\Delta\Sigma)$	-1
2	$[2,2,2] \mathbf{1}$	0	$0^+$	$\frac{1}{\sqrt{8}}(\Lambda\Lambda + 2N\Xi - \sqrt{3}\Sigma\Sigma)$	-2
3	$[3,2,1] \mathbf{8}$	$1/2$	$2^+$	$\frac{1}{\sqrt{5}}(\sqrt{2}N\Omega - \Lambda\Xi^* + \Sigma^*\Xi - \Sigma\Xi^*)$	-1

from the separate  $B$  and  $B'$   $3q$  baryons that define the lowest  $BB'$  threshold. The table shows clearly the prominence of the  $\mathcal{S} = -2$   $H$  dibaryon.

More realistic  $6q$  calculations, e.g. Refs. [7, 27], employ quark-cluster models (QCM) that break  $SU(3)_f$  and account for full quark antisymmetrization, also making contact via resonating group methods (RGM) with related  $BB'$  coupled channels and thresholds. Input interactions are shown in Fig. 3, taken from Ref. [28], where the left-hand side diagram corresponds to a gluon-exchange mediated  $BB'$  quark-exchange interaction and the right-hand side diagrams correspond to instanton induced interactions [29], a  $3q$  as well as a nonstrange  $2q$  version. Recent RGM quark calculations by Fujiwara and collaborators [30] do not use the instanton interactions, but add several meson exchanges to the gluon exchange interaction. None of these models produces a stable  $6q$  dibaryon. This may be demonstrated for the  $H$  within several frameworks, including the QCM, as follows:

- In the QCM, owing to the repulsive instanton induced interaction, the  $H$  becomes barely bound or unbound, perhaps a  $\Lambda\Lambda$  resonance below the  $N\Xi$  threshold [27].

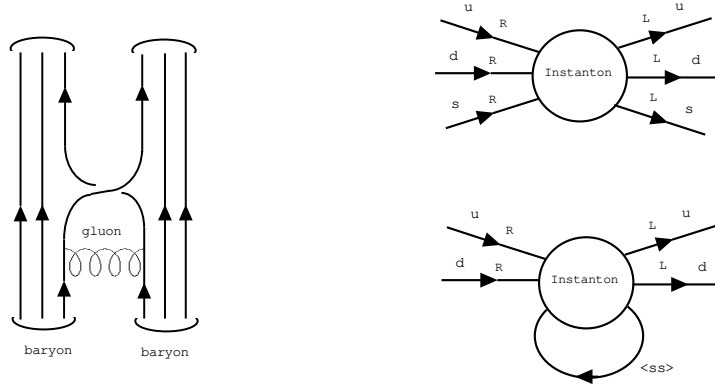


Figure 3: Quark interaction diagrams for  $6q$  dibaryon calculations [7, 28]. Left: one gluon exchange accompanied by quark exchange. Right: instanton contributions.

- In QCD sum rule calculations, where  $m_H$  is correlated with  $m_{nn}$ , the  $H$  might be bound, although with a large uncertainty,  $B_H = 40 \pm 70$  MeV [31].
- Particle stability of  ${}_{\Lambda\Lambda}^6\text{He}$  rules out  $B_H > 7$  MeV, otherwise  ${}_{\Lambda\Lambda}^6\text{He}$  would have disintegrated into  $H + {}^4\text{He}$ , at odds with its observed weak decay.

#### 4. Pion assisted dibaryons

Here we sketch the recent calculation [20] of a  $(I, J^P) = (\frac{3}{2}, 2^+)$   $\pi\Lambda N$  quasibound state, driven by the two-body  $\pi N$  resonance  $\Delta(1232)$  and the  $\pi\Lambda - \pi\Sigma$  resonance  $\Sigma(1385)$ , for a  $\Lambda N - \Sigma N$   ${}^3S_1 - {}^3D_1$  coupled channels configuration. The  $YN$  interaction was taken from a chiral QM calculation, with parameters constrained by acceptable low-energy parameters [32]. The  $\pi B$  interactions were taken in a rank-one separable form

$$\langle p | V_{\pi B, \pi B'} | p' \rangle = (\gamma_B \gamma_{B'}')^{\frac{1}{2}} g_{\pi B}(p) g_{\pi B'}(p') . \quad (3)$$

The  $\pi N \Delta(1232)$   $p$ -wave form factor  $g_{\pi N}$  was obtained from a very good fit of the  $P_{33}$  phase shift to a functional form with three well constrained



parameters (in addition to  $\gamma_{\pi N}$ ):

$$g_{\pi N}(p) = p[e^{-p^2/\beta^2} + Ap^2e^{-p^2/\alpha^2}] , \quad (4)$$

$$A = 0.2 \text{ fm}^2, \beta = 1.31 \text{ fm}^{-1}, \alpha = 3.21 \text{ fm}^{-1}. \quad (5)$$

The r.m.s. momentum associated with  $g_{\pi N}(p)$  is  $\langle p_{\pi N}^2 \rangle^{\frac{1}{2}} = 5.55 \text{ fm}^{-1} = 1095 \text{ MeV/c}$ , where

$$\langle p_{\pi N}^2 \rangle = \frac{\int_0^\infty g_{\pi N}(p) p^2 d^3p}{\int_0^\infty g_{\pi N}(p) d^3p}. \quad (6)$$

This high-momentum value does not rule out a spatial size of order 1 fm for  $\Delta(1232)$ . Indeed, if  $\tilde{g}_{\pi N}(r)$  is the Fourier transform of  $g_{\pi N}(p)$ , for  $\ell = 1$ , then  $\langle r_{\pi N}^2 \rangle^{\frac{1}{2}} = 0.875 \text{ fm}$ . The  $\pi Y \Sigma(1385)$  coupled-channel  $p$ -wave form factor was fitted to the position, width and decay branching ratios of  $\Sigma(1385)$ , using the form

$$g_{\pi Y}(p) = p(1 + Ap^2)e^{-p^2/\alpha^2} , \quad (7)$$

leaving room for gridding over one of four fit parameters which was chosen to be  $A$ . The sensitivity of the quasibound calculation to values of  $A$  in the range  $1.0 - 1.8 \text{ fm}^2$  is demonstrated by the last four columns in Table 3. It is by far the strongest sensitivity in this calculation, remarkably so for a fairly small variation over the range of r.m.s. momenta associated with the  $p$ -wave form factor  $g_{\pi Y}(p)$ .

Irrespective of which  $\pi Y$  model is chosen, the  $YN$  interaction always produces repulsion, thus lowering the calculated binding energy, as demonstrated in the last line of Table 3 which corresponds to switching off the  $YN$  interaction. This repulsive  $YN$  effect owes its origin to the high-momentum components of the  $\pi B$  form factors which within the three-body calculation highlight the short-range repulsive region of the  $YN$  interaction. All in all, the calculations described above leave sufficient room for a quasibound  $S = -1$  dibaryon, here denoted  $\mathcal{D}$ , decaying to a  $d$ -wave  $I = \frac{3}{2} \Sigma N$  scattering state and perhaps also to  $(\pi \Lambda N)_{I=\frac{3}{2}}$  if it corresponds to  $\pi \Sigma N$  quasibound state above the  $\pi \Lambda N$  threshold. To search for  $\mathcal{D}$ , the following reactions are possible:

$$K^- + d \rightarrow \mathcal{D}^- + \pi^+ , \quad \pi^- + d \rightarrow \mathcal{D}^- + K^+ , \quad (8)$$

$$p + p \rightarrow \mathcal{D}^+ + K^+ . \quad (9)$$

Table 3:  $\pi\Lambda N$  binding energy (in MeV) calculated [20] for four  $\pi Y$  interaction models specified by  $\langle p_{\pi Y}^2 \rangle^{\frac{1}{2}}$  and six chiral QM versions of the  ${}^3S_1 - {}^3D_1$   $YN$  interaction fitted to given  $\Lambda N$  scattering length  $a$  and effective range  $r_0$ . The momentum  $p_{\text{lab}}(\delta = 0)$  is the  $\Lambda$  laboratory momentum where the  ${}^3S_1$   $\Lambda N$  phase shift changes sign. The last row corresponds to switching off the  $YN$  interaction.

YN interaction			$\langle p_{\pi Y}^2 \rangle^{\frac{1}{2}}$ (fm $^{-1}$ )			
$a$	$r_0$	$p_{\text{lab}}(\delta = 0)$	3.91	3.76	3.60	3.48
(fm)	(fm)	(MeV/c)	$B_{\pi\Lambda N}$ (MeV)			
-1.35	3.39	987	99	65	30	6
-1.40	3.32	1011	99	66	30	6
-1.64	3.09	1146	102	68	32	8
-1.71	3.03	1198	102	68	33	9
-1.78	2.98	1272	103	69	33	9
-1.86	2.93	1446	104	69	34	10
-	-	-	120	84	47	21

## 5. Kaon assisted dibaryons

The low-energy  $\bar{K}N$   $s$ -wave interaction is particularly strong in the  $I = 0$  channel, leading to a  $\bar{K}N - \pi\Sigma$  QBS, the  $\Lambda(1405)$ , nominally 27 MeV below the  $K^-p$  threshold and with a decay width of about 50 MeV to the  $\pi\Sigma$  channel. The lightest  $\bar{K}NN$  dibaryon configuration maximizing the strongly attractive  $I = 0$   $\bar{K}N$  interaction is  $[\bar{K}(NN)_{I=1}]_{I=1/2, J^\pi=0^-}$ , loosely denoted as  $K^-pp$ . Several few-body calculations of  $K^-pp$  are summarized in Table 4.

Table 4: Calculated  $K^-pp$  binding energies ( $B_{K^-pp}$ ), mesonic ( $\Gamma_m$ ) & nonmesonic ( $\Gamma_{nm}$ ) widths (in MeV).

	single $\bar{K}N - \pi\Sigma$ QBS			pole		two poles
	variational		Faddeev			variational
	[33, 34]	[35]		[37]		[38]
$B_{K^-pp}$	48	40–80	50–70	44–58	9–16	17–23
$\Gamma_m$	61	40–85	90–110	34–40	34–46	40–70
$\Gamma_{nm}$	12	$\sim 20$				4–12

The table supports the expectation that the  $K^-pp$  system is bound, although there are marked differences between the values calculated for the

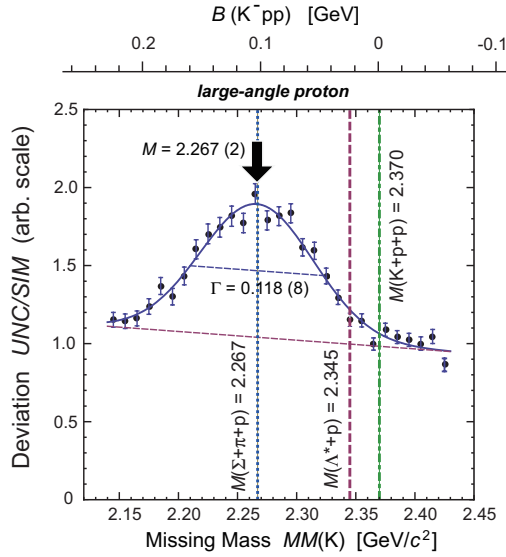


Figure 4: DISTO reanalysis of  $K^+$  missing-mass spectrum in  $pp \rightarrow K^+\Lambda p$  at  $T_p = 2.85$  GeV [41].

binding energy  $B_{K^-pp}$ . The input to all of the listed calculations is constrained by requiring that the  $\Lambda(1405)\pi\Sigma$  resonance position, and as much as possible also its shape, are reproduced. The models that achieve it with one  $\bar{K}N - \pi\Sigma$  QBS pole, necessarily at or in the immediate vicinity of  $\sqrt{s} = 1405$  MeV, produce  $K^-pp$  binding in the range 40 – 80 MeV, considerably higher than the 10 – 20 MeV range in models with two  $\bar{K}N - \pi\Sigma$  QBS poles. Among the listed calculations, only Refs. [37, 38] used chiral  $\bar{K}N - \pi\Sigma$  models that produce two such poles, but in the first listed Faddeev calculation of Ref. [37] the energy dependence of the  $\bar{K}N - \pi\Sigma$  coupled channels input was suppressed in favor of fixed threshold values, thus making it effectively a single-pole calculation.<sup>1</sup> The shallow QBS of the last two columns are primarily related to the pole position of the chiral  $\bar{K}N$  amplitude which resonates at 1420 MeV (close to the upper of the two  $\bar{K}N - \pi\Sigma$  poles) in chiral

<sup>1</sup>The second listed Faddeev calculation of Ref. [37], in addition to a relatively shallow  $K^-pp$  QBS listed in the column before last, also produced a deeply lying and very broad  $K^-pp$  QBS (unlisted in the table) in the range of  $B_{K^-pp} = (67 - 89)$  MeV and  $\Gamma_m = (244 - 320)$  MeV.

models, whereas in single-pole models the  $\bar{K}N$  amplitude resonates necessarily at 1405 MeV. This correlation with the resonance behavior of the  $\bar{K}N$  amplitude has been verified in the variational calculations of Ref. [35] and in the coupled-channel Faddeev study of Ref. [39]. A notable feature of the  $K^-pp$  single-pole coupled-channel calculations [35, 36] in Table 4 is that the explicit use of the  $\pi\Sigma N$  channel adds about  $20 \pm 5$  MeV to the  $K^-pp$  binding energy with respect to that calculated using effective  $\bar{K}N$  potential within a  $\bar{K}NN$  single-channel calculation [40].

A reanalyzed DISTO spectrum of  $pp \rightarrow K^+\Lambda p$  from Ref. [41] is shown in Fig. 4. The authors claim that the peak structure of the outgoing  $\Lambda p$  gives evidence for a  $K^-pp$  quasibound state decaying via  $K^-pp \rightarrow \Lambda p$ . The location of the peak practically on top of the  $\pi\Sigma N$  threshold, and its large width, are at odds with any of the few-body calculations listed in Table 4, posing a problem for a  $K^-pp$  QBS interpretation. At present, besides ongoing  $p(p, K^+)$  measurements at GSI to improve on the DISTO data, the  $K^-pp$  system will be explored at J-PARC in the  ${}^3\text{He}(K^-, n)$  and  $d(\pi^+, K^+)$  reactions.

## 6. Summary and outlook

In this Festschrift contribution I have reviewed the state of the art in dibaryons with strangeness, including  $K^-pp$  for which extensive experimental searches are underway. A new class of strange dibaryons which are termed meson assisted strange dibaryons was highlighted.  $K^-pp$  is just one example, where the strong  $s$ -wave  $K^-p$  interactions stabilize the initially unstable  $pp$  dibaryon. Pion assisted dibaryons  $\pi BB'$  offer more possibilities by making use of the strong  $p$ -wave  $\pi B$  and  $\pi B'$  resonances classified in the SU(3)  $\mathbf{10}_f$  representation and its extensions into charm  $\mathcal{C} \neq 0$ . Possible candidates are as follows [19].

- $\mathcal{S} \neq 0, \mathcal{C} = 0$ :

$$\mathcal{S} = -1 : \pi\Lambda N, \quad \mathcal{S} = -2 : \pi\Sigma N, \quad \mathcal{S} = -3 : \pi\Lambda\Sigma, \quad (10)$$

- $\mathcal{C} = +1$ :

$$\pi N\Lambda_c(2286), \quad \pi N\Sigma_c(2470), \quad \pi N\Omega_c(2700), \quad (11)$$

$$\pi\Lambda\Lambda_c(2286), \quad \pi\Lambda\Sigma_c(2470), \quad \pi\Lambda\Omega_c(2700), \quad (12)$$

$$\pi\Sigma\Lambda_c(2286), \quad \pi\Sigma\Sigma_c(2470), \quad \pi\Sigma\Omega_c(2700). \quad (13)$$

- $\mathcal{C} = +2$ :

$$\pi\Lambda_c(2286)\Xi_c(2470), \quad \pi\Lambda_c(2286)\Omega_c(2700), \quad \pi\Xi_c(2470)\Omega_c(2700). \quad (14)$$

Note the appearance of the  $\frac{1}{2}^+$   $\Omega_c$  baryon, of quark structure *ssc*. In the case of charmed baryons, the *p*-wave non-charmed SU(3)-**10<sub>f</sub>**  $\frac{3}{2}^+$  resonances are replaced by charmed SU(3)-**6<sub>f</sub>** members of the SU(4)-**20<sub>f</sub>** extension:

$$\Sigma(1385) \rightarrow \Sigma_c(2520), \quad \Xi(1530) \rightarrow \Xi_c(2645), \quad \Omega(1670) \rightarrow \Omega_c(2770). \quad (15)$$

Here we limited listing to  $\mathcal{C} = +1$  baryons. For a future charmed bound-state study, note that the  $\pi N\Lambda_c(2286)$  threshold lies *below*  $N\Sigma_c(2455)$ , where  $\Sigma_c(2455)$  is the lowest lying known  $\Sigma_c$ , with assumed  $J^P = \frac{1}{2}^+$ . Therefore, if  $\pi N\Lambda_c(2286)$  is bound, it will decay only by weak interactions.

Realistic calculations of pion assisted dibaryons have been reported so far only for the  $\pi\Lambda N$  system with  $(I = \frac{3}{2}, J^P = 2^+)$ , where its coupling to the higher channel  $\pi\Sigma N$  was considered while the coupling to the lower nonpionic channel  $\Sigma N$  was ignored [19, 20]. This system is a good candidate for a quasibound dibaryon either below or above the  $\pi\Lambda N$  threshold, but its precise location depends sensitively on the poorly known  $\pi\Lambda\Sigma(1385) - \pi\Sigma\Sigma(1385)$  form factor. We note that the  $\pi\Lambda N$  threshold is about 130 MeV below the  $\Sigma(1385)N$  threshold and 230 MeV below the  $\Sigma\Delta(1232)$  threshold, these latter thresholds being relevant in the discussion of the leading  $6q$   $\mathcal{S} = -1$  dibaryon configuration of Table 2. In this respect a  $\pi\Lambda N$  dibaryon, if established, is the next one in excitation energy to the lowest  $\mathcal{S} = -1$  thresholds of  $\Lambda N$  and  $\Sigma N$ .

## Acknowledgements

Gerry Brown has played a leading role in the development of nuclear physics and its derivatives. On this occasion of his 85th birthday Festschrift, I am pleased to acknowledge many inspiring suggestions he made to me throughout my own career. The work on pion assisted dibaryons is coauthored by Humberto Garcilazo who has contributed significantly to its development. I wish to also thank Wolfram Weise with whom I enjoyed several inspiring discussions on the  $K^-pp$  dibaryon and its implications to  $\bar{K}$ -nuclear physics. This research is partially supported by the EU Initiative FP7, HadronPhysics2, under Project 227431.

## References

- [1] M. Bashkanov *et al.* (CELSIUS/WASA Collaboration), Phys. Rev. Lett. **102**, 052301 (2009); P. Adlarson *et al.* (WASA@COSY Collaboration), Phys. Rev. Lett. **106**, 242302 (2011); see, however, T. Skorodko *et al.* (CELSIUS/WASA Collaboration), Phys. Lett. **B679**, 30 (2009), **B695**, 115 (2011), and S. Dymov *et al.* (COSY-ANKE Collaboration), Phys. Rev. Lett. **102**, 192301 (2009).
- [2] M. Oka and K. Yazaki, Phys. Lett. **90B**, 41 (1980).
- [3] R.L. Jaffe, Phys. Rev. Lett. **38**, 195 (1977).
- [4] B. Bassalleck, Nucl. Phys. **A639**, 401c (1998); B.A. Cole, Nucl. Phys. **A639**, 407c (1998); H.J. Crawford, Nucl. Phys. **A639**, 417c (1998).
- [5] T. Goldman, K. Maltman, G.J. Stephenson, Jr., K.E. Schmidt, and F. Wang, Phys. Rev. Lett. **59**, 627 (1987).
- [6] M. Oka, K. Shimizu, and K. Yazaki, Phys. Lett. **130B**, 365 (1983).
- [7] M. Oka, Phys. Rev. D **38**, 298 (1988).
- [8] T.H. Tan, Phys. Rev. Lett. **23**, 395 (1969); see also C. Pigot *et al.*, Nucl. Phys. **B249**, 172 (1985).
- [9] G. Toker, A. Gal, and J.M. Eisenberg, Phys. Lett. **88B**, 235 (1979); Nucl. Phys. **A362**, 405 (1981).
- [10] M. Torres, R.H. Dalitz, and A. Deloff, Phys. Lett. **B174**, 213 (1986).
- [11] P.J. Mulders, A.T. Aerts, and J.J. de Swart, Phys. Rev. D **21**, 2653 (1980); A.T. Aerts, and C.B. Dover, Phys. Lett. **B146**, 95 (1984).
- [12] K. Johnston *et al.*, Phys. Rev. C **46**, R1573 (1992).
- [13] R.E. Chrien, C.B. Dover, and A. Gal, Czech. J. Phys. **42**, 1089 (1992).
- [14] A. Budzanowski *et al.* (COSY-HIRES Collaboration), Phys. Lett. **B692**, 10 (2010).
- [15] A. Budzanowski *et al.* (COSY-HIRES Collaboration), Phys. Lett. **B687**, 31 (2010), Phys. Rev. D **84**, 032002 (2011).

- [16] R. Siebert *et al.*, Nucl. Phys. **A567**, 819 (1994).
- [17] P.J. Mulders, A.T. Aerts, and J.J. de Swart, Phys. Rev. Lett. **40**, 1543 (1978).
- [18] R. Bilger, H.A. Clement, and M.G. Schepkin, Phys. Rev. Lett. **71**, 42 (1993), **72**, 2972 (1994).
- [19] A. Gal, and H. Garcilazo, Phys. Rev. D **78**, 014013 (2008).
- [20] H. Garcilazo, and A. Gal, Phys. Rev. C **81**, 055205 (2010).
- [21] W. Weise, Nucl. Phys. **A835**, 51 (2010).
- [22] V.G.J. Stoks, and Th.A. Rijken, Phys. Rev. C **59**, 3009 (1999).
- [23] J. Haidenbauer, and U.-G. Meißner, Phys. Lett. **B684**, 275 (2010).
- [24] Th.A. Rijken, M.M. Nagels, and Y. Yamamoto, Nucl. Phys. **A835**, 160 (2010); Th.A. Rijken, and Y. Yamamoto, Nucl. Phys. **A804**, 51 (2008).
- [25] H. Polinder, J. Haidenbauer, and U.-G. Meißner, Nucl. Phys. **A779**, 244 (2006).
- [26] H. Polinder, J. Haidenbauer, and U.-G. Meißner, Phys. Lett. **B653**, 29 (2007).
- [27] S. Takeuchi, and M. Oka, Phys. Rev. Lett. **66**, 1271 (1991); M. Oka, and S. Takeuchi, Nucl. Phys. **A524**, 649 (1991).
- [28] M. Oka, Hyperfine Interactions **103**, 275 (1996) [arXiv:hep-ph/9510354].
- [29] N. I. Kochelev, Yad. Fiz. **41**, 456 (1985) [Sov. J. Nucl. Phys. **41**, 291 (1985)].
- [30] Y. Fujiwara, Y. Suzuki, and C. Nakamoto, Prog. Part. Nucl. Phys. **58**, 439 (2007).
- [31] N. Kodama, M. Oka, and T. Hatsuda, Nucl. Phys. **A580**, 445 (1994).
- [32] H. Garcilazo, T. Fernández-Carames, and A. Valcarce, Phys. Rev. C **75**, 034002 (2007); H. Garcilazo, A. Valcarce, and T. Fernández-Carames, Phys. Rev. C **76**, 034001 (2007).

- [33] T. Yamazaki, and Y. Akaishi, Phys. Lett. **B535**, 70 (2002).
- [34] Y. Akaishi, and T. Yamazaki, Phys. Rev. C **65**, 044005 (2002) [Eq. (29)].
- [35] S. Wycech, and A.M. Green, Phys. Rev. C **79**, 014001 (2009).
- [36] N.V. Shevchenko, A. Gal, and J. Mareš, Phys. Rev. Lett. **98**, 082301 (2007).
- [37] Y. Ikeda, H. Kamano, and T. Sato, Prog. Theor. Phys. **124**, 533 (2010).
- [38] A. Doté, T. Hyodo, and W. Weise, Nucl. Phys. **A804**, 197 (2008), Phys. Rev. C **79**, 014003 (2009).
- [39] N.V. Shevchenko, A. Gal, J. Mareš, and J. Révai, Phys. Rev. C **76**, 044004 (2007).
- [40] Y. Ikeda, and T. Sato, Phys. Rev. C **79**, 035201 (2009); see also Y. Ikeda, and T. Sato, Phys. Rev. C **76**, 035203 (2007).
- [41] T. Yamazaki *et al.*, Phys. Rev. Lett. **104**, 132502 (2010).